

1 **A homozygous hypomorphic *BRCA2* variant causes primary ovarian insufficiency without**  
2 **cancer or Fanconi anemia traits.**

3

4 Sandrine Caburet<sup>1,#</sup>, Abdelkader Heddar<sup>2,#</sup>, Elodie Dardillac<sup>3,4,#</sup>, Helene Creux<sup>5</sup>, Marie  
5 Lambert<sup>5</sup>, Sébastien Messiaen<sup>6</sup>, Sophie Tourpin<sup>6</sup>, Gabriel Livera<sup>6</sup>, Bernard S. Lopez<sup>3,4,\*</sup>,  
6 Micheline Misrahi<sup>2,\*</sup>

7

8 <sup>1</sup> Université de Paris, Institut Jacques Monod, CNRS UMR7592, F-75013 Paris, France.

9 <sup>2</sup> Faculté de Médecine, Universités Paris-Sud-Paris-Saclay, Hôpital Bicêtre, 94275, Le Kremlin  
10 Bicêtre, France.

11 <sup>3</sup> Institut Cochin, INSERM U1016, UMR 8104 CNRS, Université de Paris, 75014 Paris, France.

12 Team labeled by “Ligue Nationale contre le cancer, Ligue 2017”.

13 <sup>4</sup> CNRS UMR 8200, Institut de Cancérologie Gustave-Roussy, Université Paris-Saclay,  
14 Villejuif, France.

15 <sup>5</sup> Service de Gynécologie et Médecine de la Reproduction, CHU de Bordeaux, 33000, France.

16 <sup>6</sup> UMR Stabilité Génétique, Cellules Souches et Radiations, Université de Paris, Université  
17 Paris-Saclay, CEA/DRF/iRCM/SDRR/LDG, 18 route du Panorama, Fontenay aux Roses, F-  
18 92265, France.

19

20 # These authors contributed equally to this work.

21 \* Corresponding author: [micheline.misrahi@aphp.fr](mailto:micheline.misrahi@aphp.fr).

22 \* Corresponding author: [bernard.lopez@inserm.fr](mailto:bernard.lopez@inserm.fr).

23

24 **Running title:** Mutant *BRCA2* in isolated ovarian insufficiency.

25 **ABSTRACT**

26 Primary Ovarian insufficiency (POI) affects 1% of women under forty. We studied a patient  
27 with a non-syndromic POI, from a consanguineous Turkish family. Exome sequencing  
28 identified a homozygous missense variant c.8524C>T/p.R2842C in *BRCA2*. *BRCA2* is a major  
29 player in homologous recombination (HR). *BRCA2* deficiency induces cancer predisposition  
30 and Fanconi Anemia (FA). Remarkably, neither the patient nor her family exhibit somatic  
31 pathologies. The patient's somatic cells presented intermediate levels of chromosomal breaks,  
32 cell proliferation and radiation-induced RAD51 foci formation when compared to controls, the  
33 heterozygous mother's and FA cells. R2842C-*BRCA2* partially complemented *BRCA2*  
34 depletion for double-strand break-induced HR. The residual HR function in patient's cells could  
35 explain the absence of somatic pathology. *BRCA2* is expressed in human fetal ovaries in  
36 pachytene stage oocytes, when meiotic HR occurs. This study has a major impact on the  
37 understanding of genome maintenance in somatic and meiotic cells and on the management of  
38 POI patients.

39

40 **Keywords:** *BRCA2* / mutation / cancer / Fanconi anemia / Primary ovarian insufficiency /  
41 meiosis.

42

## 43 INTRODUCTION

44 Primary ovarian insufficiency (POI) is a public health issue affecting ~1% of women under 40  
45 years, and is clinically heterogeneous with isolated or syndromic forms (Huhtaniemi et al.,  
46 2018). Most cases are idiopathic but an increasing number of genetic causes have been recently  
47 identified, especially mutations in genes involved in DNA repair and recombination (AlAsiri et  
48 al., 2015; Fouquet et al., 2017; Wood-Trageser et al., 2014).

49 DNA repair and recombination are essential for genome maintenance. The DNA damage  
50 response (DDR) coordinates a network of pathways insuring faithful transmission of genetic  
51 material. Consistently, defects in the DDR result in genome instability associated with  
52 developmental anomalies and cancer predisposition (Hoeijmakers, 2009). Homologous  
53 recombination (HR), an evolutionary conserved process essential to genome stability and cell  
54 viability, plays crucial roles in DNA double strand break (DSB) repair in somatic and meiotic  
55 cells.

56 In mammals, BRCA2 binds damaged DNA and loads the pivotal HR player RAD51, which then  
57 promotes DNA homology search. Therefore, cells defective in RAD51 or BRCA2 are thus  
58 defective in mitotic HR (Lambert and Lopez, 2000; Moynahan et al., 2001). Heterozygous  
59 *BRCA2* mutations increase susceptibility to breast and ovarian cancers, whereas severe bi-allelic  
60 defects in *RAD51* (*FANCR*) or *BRCA2* (*FANCD1*) lead to Fanconi anemia (FA) syndrome (Tsui  
61 and Crismani, 2019). In particular, *FANCD1* syndrome associates developmental defects,  
62 genetic instability, bone marrow failure and cancer predisposition, with cancer developing in  
63 the first decade of life, and death before puberty (Meyer et al., 2014). The role of BRCA2 in  
64 RAD51 loading in mitotic HR makes it a strong candidate for an involvement in meiotic HR,  
65 but this remains to be formally established. Indeed, the severe phenotypes of bi-allelic  
66 inactivation of BRCA2 in humans and the early embryonic lethality resulting from germ-line  
67 inactivation of this essential gene in animal models hampered meiosis analysis and

68 compromised the study of the putative functions of BRCA2 in gametogenesis (Ludwig et al.,  
69 1997; Sharan et al., 1997; Tsuzuki et al., 1996).

70 We describe here an adult patient carrying a homozygous missense mutation in *BRCA2* with  
71 isolated POI, but without cancer nor FA traits in the patient or her family. We demonstrate that  
72 the mutated R2842C-*BRCA2* retains a lower but significant residual function when compared  
73 to wild-type (WT)-*BRCA2*. Consistently, the patient's cells exhibit intermediate levels in  
74 chromosomal breaks, cell proliferation and ionizing radiation-induced RAD51 foci formation  
75 when compared to controls, a FANCD1 patient's or the heterozygous mother's cells. This  
76 residual HR in somatic cells could explain the absence of *in vivo* somatic pathologies. *BRCA2*  
77 is a major cancer susceptibility gene and our finding will have a strong impact on the genetic  
78 counselling and management of patients with POI and their relatives.

79

## 80 **RESULTS**

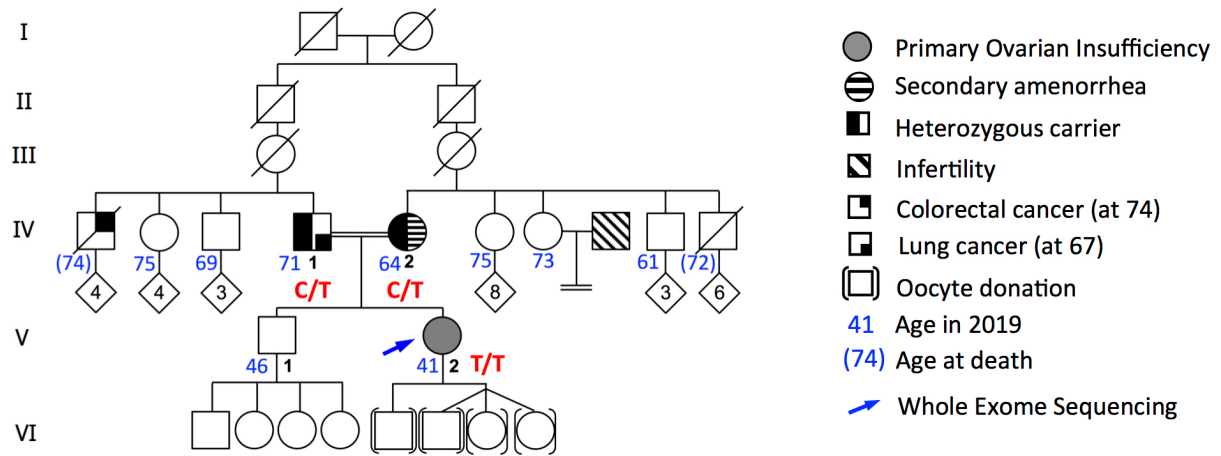
### 81 **Case report**

82 The proposita was born to consanguineous Turkish parents (Figure 1). At 13 years, she had two  
83 vaginal bleedings followed by primo-secondary amenorrhea. She had normal pilosity, breast  
84 development and external genitalia. Several hormonal assays confirmed POI and pelvic  
85 ultrasonographical studies showed small ovaries with no or very few follicles (Table 1). Blood  
86 counts, liver and thyroid balances were normal. Thyroid auto-antibodies were undetectable.  
87 Bone densitometry at 30 years showed a marked osteopenia (T score = -2.3). She is presently  
88 41 years old, displays normal blood assays and no other clinical sign. The karyotype is 46, XX  
89 and FMR1 premutation screening was negative. After two egg-donation procedures, she had  
90 two pregnancies with four healthy children.

91

92





93

94 **Figure 1: Pedigree of the Turkish family.** Double lines indicate consanguineous union. The

95 proband (blue arrow) was analysed by WES. The genotypes for the mutated codon of *BRCA2*

96 are indicated in red.

97

98 The patient and family members have a normal stature, normal head circumferences with no

99 abnormality in skin pigmentation, skeletal development or dysmorphia (Table 1). There was no

100 familial history of infertility or other diseases. The mother married at the age of 15 and had two

101 pregnancies at 18 (a boy) and 22 years (the proband). This is in line with a delayed conception

102 followed by secondary amenorrhea at the age of 33, not investigated in Turkey. She is obese

103 with a BMI of 38. In order to rule out other genetic causes that could explain her subfertility,

104 we performed a targeted NGS (see supplementary information). The brother had one healthy

105 son (17 years) and 3 healthy daughters aged 15, 13 (both with normal puberty) and 8 years. The

106 71 years-old father, a heavy smoker, had a lung cancer at the age of 67 years, treated by

107 radiotherapy and chemotherapy. A paternal uncle developed a colorectal cancer at the age of 74

108 years and died few months later. Six other paternal and maternal uncles and aunts are 61 to 75

109 years old and have no history of cancer or infertility.

110

Case	Menstrual cycles	Age at evaluation (years)	BMI (height cm/weight kg)	Head circumference cm (SD)	(R/L) Ovarian Volume mm <sup>3</sup>	(R/L) Follicle number	FSH IU/l	LH IU/l	E2 nmol/l	AMH ng/ml	InhB ng/l	T nmol/l	PRL ng/ml	TSH mU/l
Index	Primo-Secondary amenorrhea (13 years)	30	23 (156/55)	55.5 (0)	21/17	2/0	85	16.7	0.04			0.5	17.5	1.45
		32			0.9/0.5									
		39	24 (156/58)		19/17	0/0	113	36.5	0.08				0.6	29.5
Mother	Secondary amenorrhea (33 years)	63	38 (155/90)	56 (0)	Normal ranges	Follicular phase	2.9-12	1.5-8	0.06-0.54	2.2 - 6.8	10 - 320	0.4 - 2	0.7 - 25	0.3 - 4.2
						Ovulatory phase	6.3-24	9.6-80	0.16-0.78					
						Luteal phase	1.5-7	0.2-6.5	0.34-2.1					
						Menopause	17-95	8-33	≤0.2					
Father		70	17 (170/50)	55 (0)										
Brother		45	28 (171/80)	57 (0)										

1

112 **Table 1: Clinical and biological studies of the proband and relatives.**

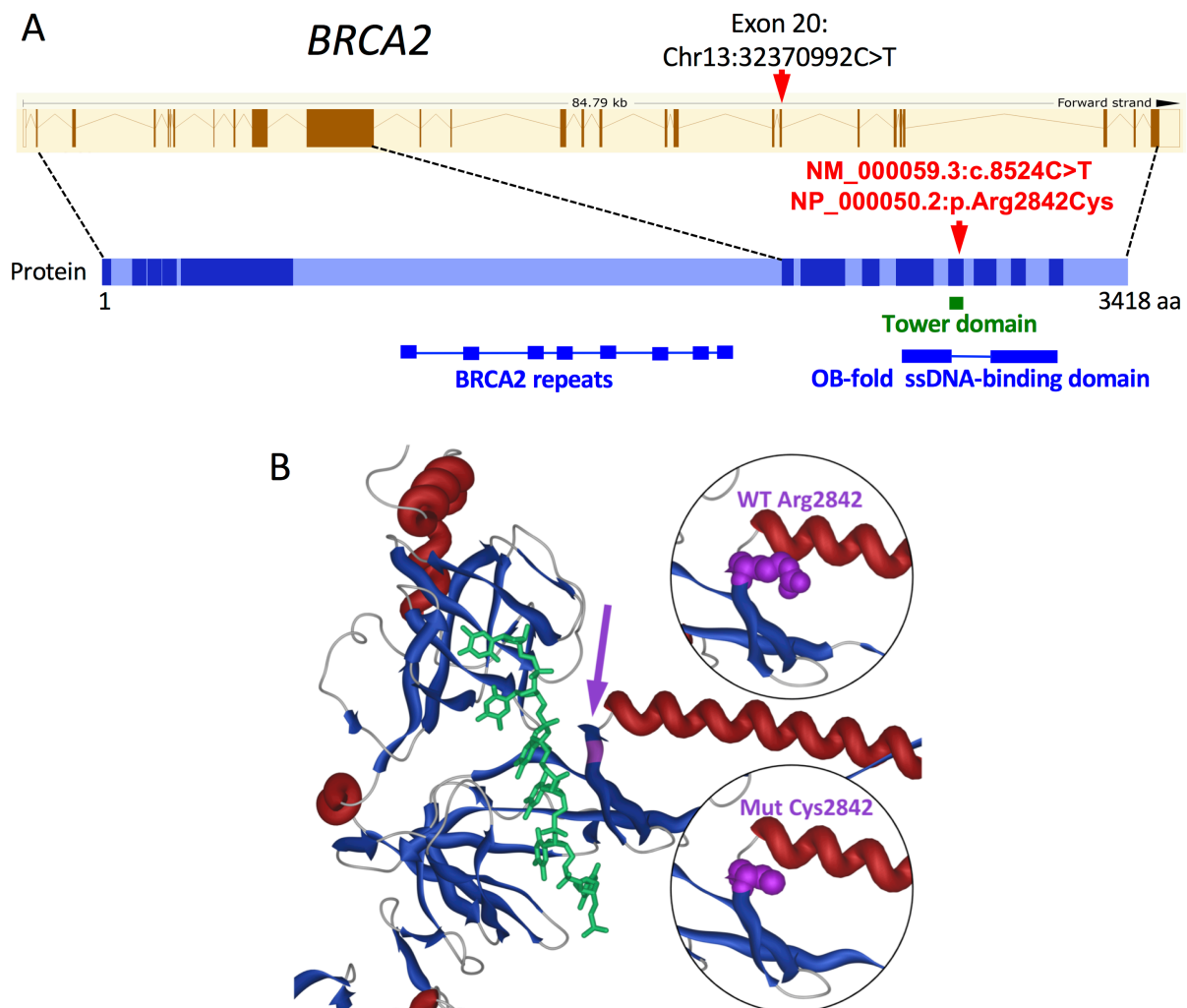
113 BMI: body mass index; SD: deviation compared to standards; R: Right; L: Left; FSH: Follicle-  
 114 stimulating hormone; LH: Luteinizing hormone; E2: estradiol; AMH: anti-Müllerian hormone;  
 115 InhB: inhibine B; T: testosterone; PRL: prolactin; TSH: thyroid-stimulating hormone.

116

117 **Whole-exome sequencing identified a homozygous missense variant in the DNA-binding**  
 118 **domain of *BRCA2***

119 The patient was studied by whole-exome sequencing (WES). Familial consanguinity suggested  
 120 an autosomal recessive inheritance pattern. The variants were therefore filtered on the basis of  
 121 their homozygosity in the patient, their absence in unrelated fertile in-house controls and a minor  
 122 allele frequency (MAF) below 0.01 in all available databases. Further filtering on available  
 123 functional data for a possible role in fertility revealed the missense variant rs80359104,  
 124 NM\_000059.3: c.8524C>T (p.R2842C), located in exon 20 of *BRCA2* (Figure 2A, Figure 2–  
 125 figure supplement 1 and Figure 2–figure supplement 2). The variant is very rare and presents  
 126 only at the heterozygous state in 3 out of 138342 individuals without known phenotype (MAF  
 127  $1.10^{-5}$ ) in the non-cancer GnomAD subset. It is absent in the Greater Middle East Variome  
 128 database dedicated to Middle Eastern populations. It is predicted to be pathogenic by 16 of 17  
 129 predictive softwares (Figure 2–figure supplement 3).

130 The variant changes a strictly-conserved aminoacid (aa) at the base of the Tower part of the  
131 BRCA2 DNA-binding domain, in close proximity to the groove that binds single-stranded DNA  
132 (ssDNA) (Figure 2B and Figure 2-figure supplement 4). This C-terminal domain is essential  
133 for appropriate binding of BRCA2 to ssDNA (Yang et al., 2002).  
134



135  
136 **Figure 2: Mutation of *BRCA2* in a POI patient without FA trait.** **A.** Position of the variant  
137 in *BRCA2* gene and protein. The structure of the normal protein for the longest isoform of 3418  
138 residues is shown below the genomic structure with the coding exons as coloured bars (Ensembl,  
139 reference transcript ENST00000544455.5). The mutation (red arrow) lies at the very end of  
140 exon 20, which encodes 48 aminoacids (aa) encompassing the Tower domain at the center of  
141 the OB-fold ssDNA-binding domain (oligonucleotide/oligosaccharide -Binding single-strand  
142 DNA-binding domain). **B.** Partial view of the 3D model of the BRCA2 C-terminal domain  
143 (alpha-helices in red, beta-sheets in blue). The mutated position (purple) is located near the

144 ssDNA (green), at the base of the Tower domain, that forms a stem of two long alpha-helices  
145 and a helix-turn-helix motif, similar to the DNA-binding domains of recombinases and  
146 homeodomain transcription factors. Inserts: difference between the occupancy of the lateral  
147 chain of wild-type (WT, top) and mutated (bottom) residue at this position.

148

149 [Figure 2–figure supplement 1](#): WES metrics for the POI patient

150 [Figure 2–figure supplement 2](#): Filtering of the variants identified in the POI patient

151 [Figure 2–figure supplement 3](#): Pathogenicity predictions for the R2842C variant in BRCA2

152 [Figure 2–figure supplement 4](#): Conservation of the mutated Arg 2842 across species.

153

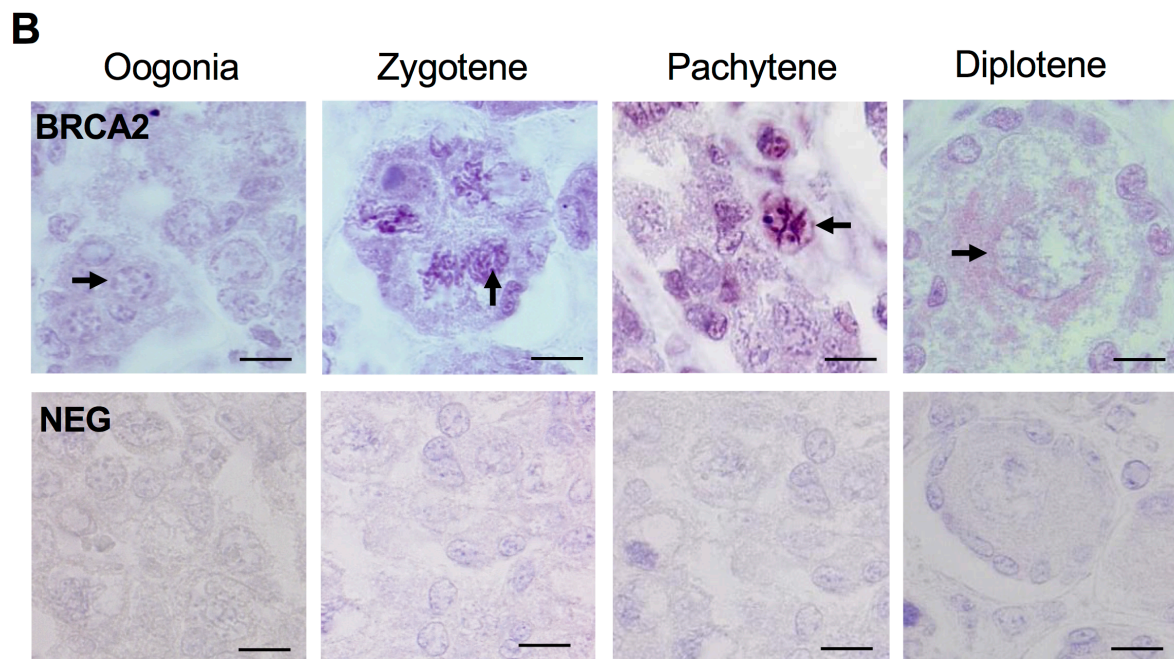
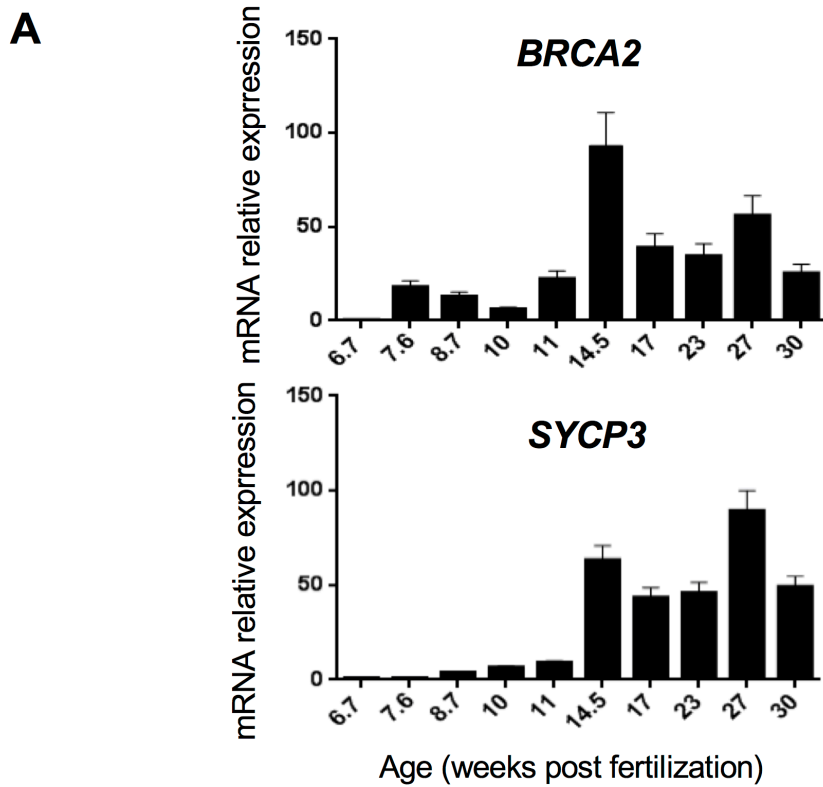
154 BRCA2 loads recombinases on ssDNA: RAD51 in mitotic cells, RAD51 and the meiotic DMC1  
155 in germ cells, indicating a crucial role for BRCA2 in mitotic and meiotic HR (Martinez et al.,  
156 2016). Cells defective in RAD51 or BRCA2 are defective in mitotic HR (Lambert and Lopez,  
157 2000; Moynahan et al., 2001) and in mouse, germ cells-specific *Brca2* deletions lead to meiotic  
158 impairment and infertility (Miao et al., 2019; Sharan et al., 2004). Therefore, we considered  
159 *R2842C-BRCA2* as a very likely causal variant for isolated POI in our patient, although she does  
160 not present FA traits. Hence, we investigated the expression of *BRCA2* in human oocytes and  
161 the functional impact of the variant on HR in human cells.

162

### 163 ***BRCA2* is expressed during meiotic prophase I in human fetal ovaries.**

164 In order to support a possible role for BRCA2 in female meiotic HR that would explain this  
165 patient's infertility, we verified its expression and localisation in human fetal ovaries. Indeed,  
166 *Brca2* mRNA expression was reported in murine oocytes (Sharan et al., 2004) and BRCA2 was  
167 described to form recombination nodule-like foci along chromosome axes in human  
168 spermatocytes (Chen et al., 1998), but its expression during human female meiosis remained  
169 undocumented. Using qRT-PCR on RNA libraries prepared from human ovarian samples at  
170 various fetal stages, we detected a predominant expression of *BRCA2* mRNA after 11 weeks  
171 post-fertilization, when oocytes enter and progress through meiotic prophase I (Figure 3A).

172 Immunostaining of human fetal ovarian sections showed that BRCA2 protein was detected  
173 mostly in pachytene stage oocytes (Figure 3B). BRCA2 staining appeared as thick threads,  
174 likely corresponding to meiotic chromosomes. These results show that BRCA2 is indeed present  
175 on chromosomes in fetal human oocytes when meiotic DSB repair occurs.



176

177 **Figure 3: BRCA2 expression in human fetal ovaries.** **A.** *BRCA2* mRNA was quantified by  
178 RT-qPCR from total RNA of pooled human fetal ovaries from various developmental stages  
179 (above). Beta-actin was used as a reference and expression is provided as percentage of the  
180 maximum. Each RNA library was analysed in triplicate and the bar indicates the mean.  
181 Quantification of *SYCP3* mRNA is shown at the same stages for comparison (below). **B.**  
182 *BRCA2* immunostaining (purple) in the cortex of a 24 weeks post fertilization human ovary.  
183 Meiotic chromosomes are stained in zygotene and pachytene stage oocytes. No staining is  
184 observed when immunohistochemistry is performed in the absence of primary antibody (NEG).  
185 Arrowheads point to germ cells at the indicated stage. Scale bar: 10  $\mu$ m.

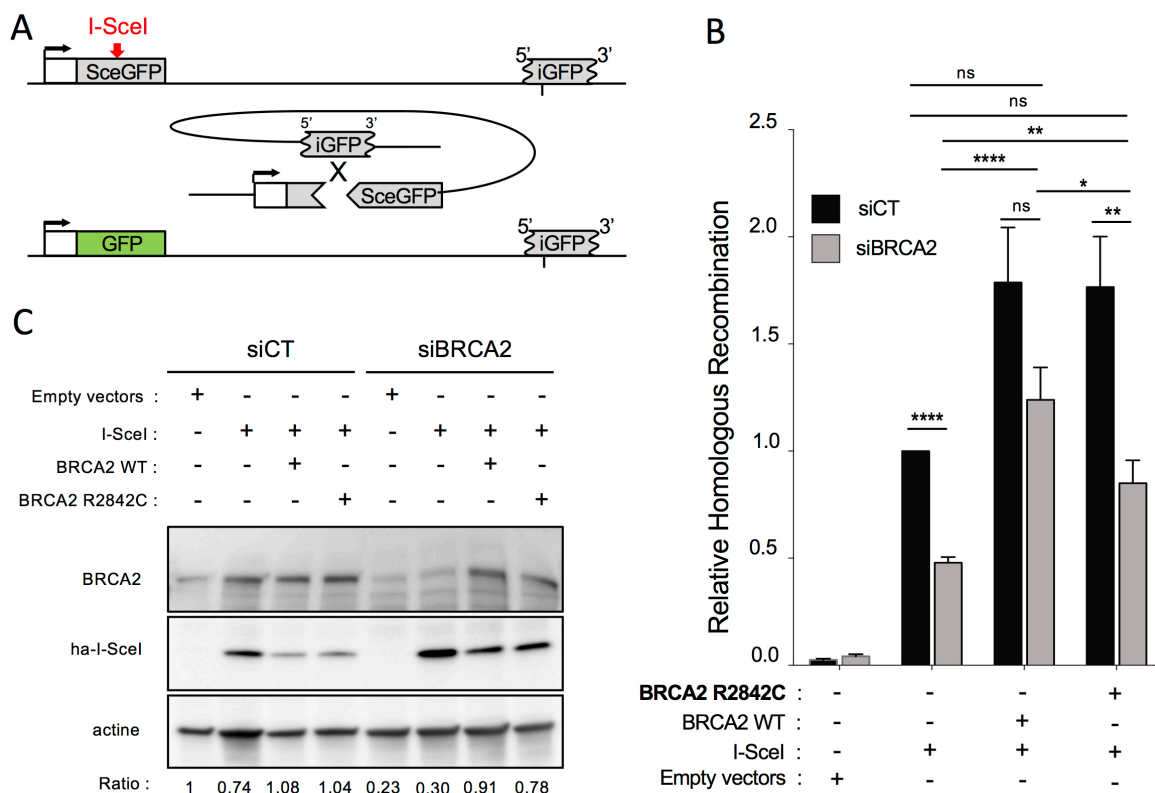
186

### 187 ***R2842C-BRCA2* displays a reduced DSB-induced HR efficiency**

188 Although referenced in the COSMIC database of variants in cancer (COSM23938), *R2842C-*  
189 *BRCA2* is considered as a variant of unknown significance for breast cancer predisposition  
190 (VUS, IARC class 3). Attempts to classify *BRCA2* VUS in a hamster lung fibroblast cell line  
191 showed that this variant displayed a little decrease in HR efficiency, at the limit for inferring  
192 pathogenicity (Guidugli et al., 2013). Therefore, the significance of this variant and its  
193 classification as a causal mutation for human pathology remained unclear. A previous attempt  
194 to classify *BRCA2* VUS in a hamster lung fibroblast cell line showed that this variant displayed  
195 a little decrease in HR efficiency, at the limit for inferring pathogenicity (Guidugli et al., 2013).  
196 Since human and rodent cells differ in their regulation of DSB repair, we analysed the specific  
197 impact of *R2842C-BRCA2* on HR in human cells. We used the RG37 cell line (Dumay et al.,  
198 2006), a human SV40 immortalized fibroblast line bearing the DR-GFP substrate (Pierce et al.,  
199 1999) that monitors gene conversion induced by targeted cleavage by the I-SceI meganuclease  
200 (Figure 4A). Both the expression of WT-*BRCA2* and *R2842C-BRCA2* stimulated the efficiency  
201 of DSB-induced HR (Figure 4B). We then silenced the endogenous *BRCA2* using a specific  
202 siRNA targeting its 3'UTR sequence, and complemented these cells with either the WT or  
203 mutated *BRCA2* (Figure 4C). As expected, silencing endogenous *BRCA2* decreased HR  
204 efficiency, and WT-*BRCA2* fully complemented HR efficiency. *R2842C-BRCA2*, expressed at



205 similar levels than WT-BRCA2, only partially complemented HR efficiency, to  $67 \pm 6\%$   
 206 compared to WT-BRCA2 (Figure 4B).  
 207 These data show that the *R2842C-BRCA2* mutation affects HR efficiency in human cells, but  
 208 only partially. This significant residual activity could account for the absence of somatic  
 209 pathology in the patient.  
 210



211  
 212 **Figure 4: Impact of the *R2842C-BRCA2* mutation on homologous recombination induced**  
 213 **by targeted DSB.** **A.** Schematic representation of the DR-GFP substrate for the study of  
 214 homologous recombination. Two inactive GFP (iGFP and SceGFP) genes are organized into  
 215 direct repeats. The I-SceI meganuclease generates a targeted DSB cleavage into the substrate  
 216 (red). HR between the two GFP genes generates a functional GFP. The DR-GFP substrate is  
 217 stably integrated in the SV40-transformed fibroblasts RG37 cell line, and the relative HR  
 218 efficiency is quantified as the fraction of GFP-positive cells (i.e. with a repaired GFP gene after  
 219 targeted cleavage). **B.** HR efficiency, measured by the fraction of GFP+  
 220 cells, in cells expressing the WT or mutated BRCA2 protein (normalised to I-SceI transfected

221 cells), and transfected either with a control siRNA (siCT) or a siRNA targeting the 3'UTR of  
222 endogenous *BRCA2* mRNA (siBRCA2). The values are normalised to the control and represent  
223 the average  $\pm$  SEM (p-values from Mann-Whitney test) for at least 3 independent experiments.  
224 **C. Expression of endogenous BRCA2 and exogenous WT-BRCA2 and R2842C-BRCA2.**  
225 Twenty micrograms of total proteins extracted from a wild type or R2842C mutant BRCA2-  
226 expressing cell line were electroblotted in the presence of endogenous BRCA2 (siCT) or after  
227 specific silencing (siBRCA2). For each condition, the expression of I-SceI and BRCA2 and the  
228 efficiency of silencing were measured. We used  $\beta$ -actin as a loading control. Below: relative  
229 quantification of BRCA2 versus actin by quantification of bands intensity with ImageJ.

230

### 231 **Increased chromosomal instability in the patient's cells**

232 Then we studied mitomycin C (MMC)-induced chromosomal breaks in lymphoblastoid cells  
233 derived from the patient, her mother, two fertile control women and a FANCD1 patient. In the  
234 absence of MMC, few spontaneous breaks were observed in cells from the proposita and the  
235 FANCD1 patient (Figure 5A and 5B). Upon exposure to 300 nM MMC, all FANCD1 cells  
236 presented breaks, as expected, while the patient's cells exhibited a slight increase of  
237 chromosomal breaks, compared to the heterozygous mother's and the WT control cells.  
238 Furthermore, at high MMC dose (1000 nM), while breaks in FANCD1 cells were too numerous  
239 to be quantified, the patient's cells presented only a modest increase of breaks (Figure 5B).  
240 These data show that the patient's cells display levels of chromosomal breaks intermediate  
241 between those of WT and FANCD1 cells.

242

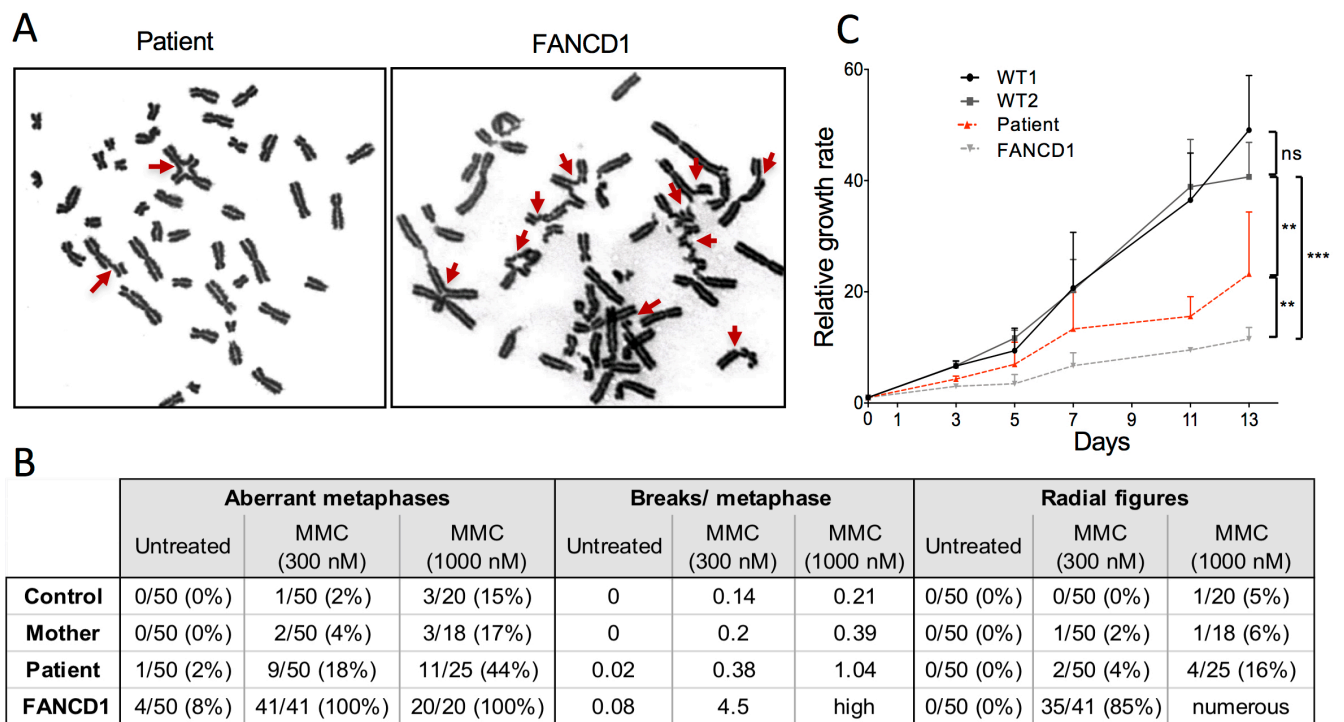
### 243 **Reduced proliferation rate of the patient's primary fibroblasts**

244 Then we compared the proliferation rate of primary fibroblasts from the POI patient, WT  
245 controls and a FANCD1 patient. As expected, the proliferation of FANCD1 cells was markedly  
246 affected when compared to that of the WT cells (Figure 5C). Remarkably, the patient's  
247 fibroblasts exhibited a moderately reduced proliferation rate, intermediate between the WT and  
248 the FANCD1 cells.



249

250



251

252 **Figure 5: Increased chromosomal instability and reduced proliferation rate in the**

253 **patient's cells. A.** Chromosomal breaks analysis of lymphoblastoid cell lines. Metaphases in

254 the patient's and FANCD1 cells in the presence of 300 nM Mitomycin C (MMC). Chromosomal

255 breaks and radial figures are shown (arrows). **B.** Quantification of chromosomal breaks in

256 lymphoblastoid cell lines derived from the patient, the mother, a *FANCD1* patient and a WT

257 control, in the absence or in the presence of MMC. **C.** Reduced proliferation rate of the patient's

258 primary fibroblasts. Cells from the POI patient, two WT controls (WT1 and WT2) and a

259 FANCD1 patient were cultured into 6-wells plates and counted every 2-3 days during thirteen

260 days. The value corresponds to the mean + SEM of at least 3 independent experiments. The

261 statistical significance was calculated from rope comparison of linear regression of growth

262 curves.

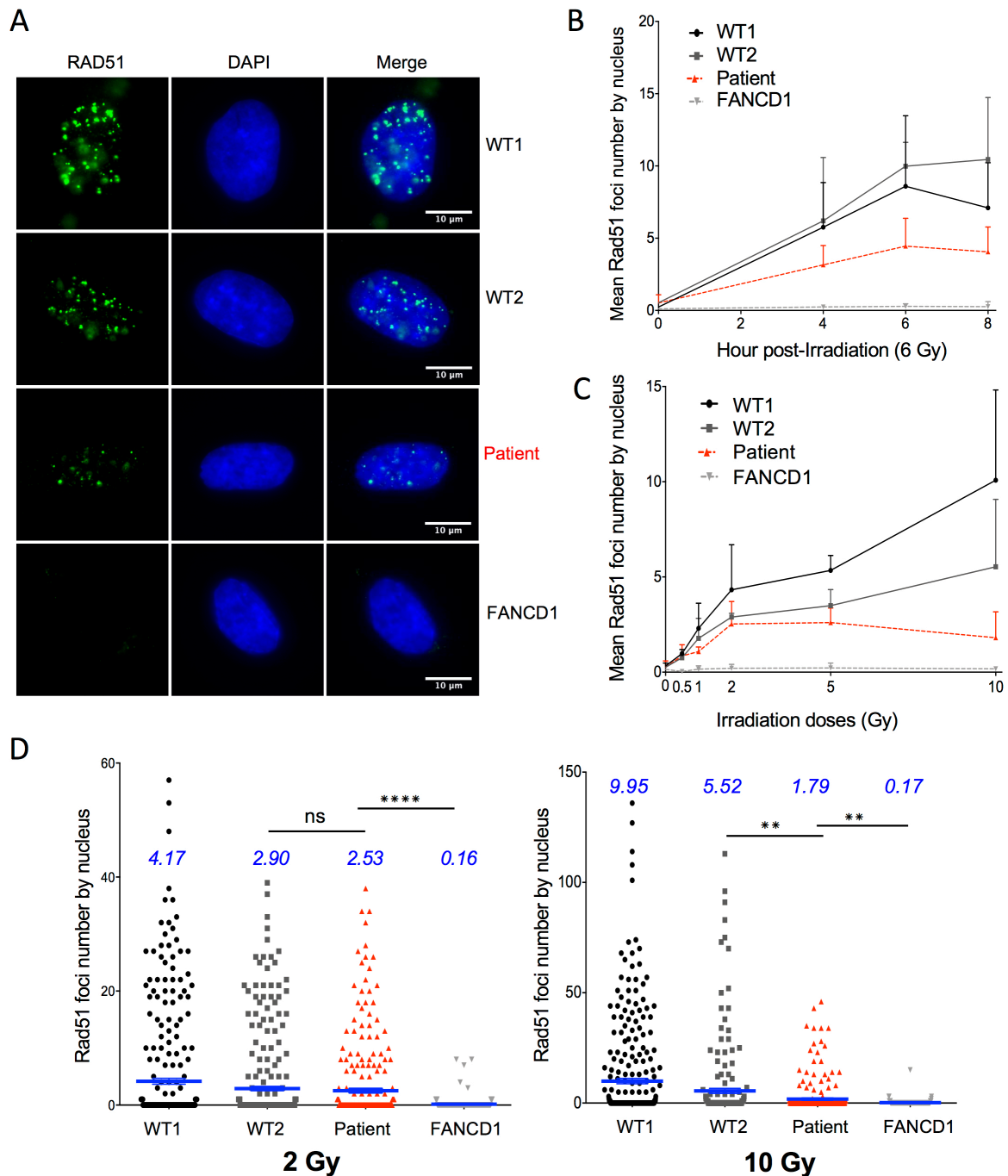
263

264 **Altered radiation-induced RAD51 foci formation in the patient's fibroblasts**

265 The main role for BRCA2 is the loading of the pivotal RAD51 recombinase on damaged DNA,

266 a crucial step for triggering HR. Therefore, we monitored the radiation-induced assembly of

267 RAD51 foci, which are considered sites of HR initiation events. As expected, FANCD1 cells  
268 failed to assemble RAD51 foci (Figure 6A and 6B). The patient's cells showed an intermediate  
269 phenotype: indeed, at 6 Gy, they assemble foci with kinetics comparable to WT cells, but the  
270 level of the plateau was about two-fold lower than in WT cells (Figure 6B). A dose-response  
271 analysis confirmed the complete deficiency in RAD51 foci assembly in FANCD1 cells, at all  
272 irradiation doses (Figure 6C and 6D). In the patient's cells, the number of RAD51 foci increased  
273 up to 2 Gy similarly to WT cells, but did not further increased at higher doses (Figure 6C, Figure  
274 6D left panel). Consequently, the patient's cells showed lower levels of RAD51 foci at high  
275 doses (>2 Gy) when compared to WT cells (Figure 6C, Figure 6D right panel). Together, these  
276 data show a dose-dependent sensitivity in the patient's cells, able to process low levels of DNA  
277 damage, but failing to assemble RAD51 foci when faced with high levels of damage.



278

279 **Figure 6: Dose-sensitive alteration of RAD51 foci formation in the patient's cells. A.**

280 RAD51 nuclear foci assembly in irradiated primary fibroblasts from the patient, two WT

281 controls and a FANCD1 patient (6 Gy, 6 hours). Fixed and permeabilised cells were probed

282 with an anti-RAD51 antibody. **B.** Kinetics of RAD51 foci assembly (6 Gy) in irradiated primary

283 fibroblasts. **C, D.** Dose response of RAD51 foci assembly (6h post-irradiation) in irradiated

284 primary fibroblasts. **C.** Complete dose response of RAD51 foci per nucleus; **D.** RAD51 foci at

285 low (2 Gy, left panel) and high (10 Gy, right panel) levels of irradiation respectively (medians

286 are in blue (n=3)). In B and C, the values correspond to the mean + SEM (n=3); p-values (stars)  
287 were obtained with Mann-Whitney test.

288

289 [Figure 6-figure supplement 1](#): Compilation of WES data for all genes involved in the FA  
290 pathway

291

292 Bi-allelic mutations in two distinct genes of the FA pathway can be found in a single individual  
293 (Singh et al., 2009). In order to rule out that the cellular phenotypes observed in the patient's  
294 cells could be due to mild bi-allelic mutations in FA genes other than *BRCA2*, we have analysed  
295 the variants found by WES in the 26 other FA genes. The good coverage of each gene, the  
296 presence of heterozygous variants (both in coding regions and in UTRS or intronic regions) and  
297 unbiased allelic ratios exclude the possibility of having missed a pathogenic variant in another  
298 FA gene (Figure 6-figure supplement 1). This analysis supports the fact that the cellular  
299 phenotypes observed in the patient's cells are not due to mutations in FA genes other than  
300 *BRCA2*. In particular, no variants in *RAD51* could explain the defects in foci assembly detected  
301 in the patient's cells.

302

### 303 **Discussion**

304 We report here for the first time a *BRCA2* homozygous hypomorphic mutation in a patient with  
305 POI, and, remarkably, without cancer nor Fanconi anemia traits in the patient and her family.  
306 The mutation is located in the ssDNA-binding domain of *BRCA2*. We performed a thorough  
307 functional study and showed that the R2842C-*BRCA2* mutant displays a reduced residual HR  
308 activity. Consistently, the patient's cells exhibit a reduced rate of proliferation, a slight increase  
309 in MMC-induced chromosomal breaks and a dose-sensitive alteration of radiation-induced  
310 assembly of *RAD51* foci. However, despite these moderate alterations in somatic cells, the  
311 patient did not develop somatic pathology, unlike *FANCD1* patients.

312 Meiotic recombination is a complex and highly regulated process occurring in meiotic  
313 prophase I and involving specific meiotic genes such as *DMC1* and *MEIOB* (Crickard et al.,  
314 2018; Souquet et al., 2013; Yoshida et al., 1998). While the role and clinical impact of  
315 homozygous and heterozygous *BRCA2* variants in mitotic cells is widely studied, the impact of  
316 such defects in human germ cells remains less understood because almost all FANCD1 patients  
317 die before puberty. However, it was very recently shown in mouse models that oocyte-specific  
318 *Brca2* defects lead to meiotic impairment, germ cells depletion and infertility (Miao et al., 2019;  
319 Tsui and Crismani, 2019). Here, we show that BRCA2 mRNA and protein are expressed in  
320 human fetal ovaries in pachytene stage oocytes, when meiotic HR occurs. Taken together, our  
321 data strongly support an actual role of BRCA2 in meiotic HR, and therefore a likely impact of  
322 R2842C-BRCA2 reduced activity on this process in our POI patient.

323 The main role of BRCA2 is the loading of the pivotal recombinase RAD51 on damaged DNA,  
324 to allow for repairing DSBs by HR. Using a HR reporter assay and quantification of RAD51  
325 foci in the patient's irradiated somatic cells, we show here that the R2842C-BRCA2 mutant  
326 exhibits a reduced DSB-induced HR efficiency, but that RAD51 foci assembly was not affected  
327 at low irradiation doses. In addition, the patient's cells displayed a growth rate and levels of  
328 chromosomal breaks intermediate between FANCD1 cells and WT cells. This shows that the  
329 patient's somatic cells are slightly altered when compared to WT cells, but at a level insufficient  
330 to cause somatic pathological consequences. Since R2842C-BRCA2 cells efficiently load  
331 RAD51 on low numbers of DNA damage, the residual HR activity of the R2842C-BRCA2  
332 mutant could account for the absence of somatic disorders.

333 Meiotic recombination in germ cells is initiated by hundreds of DSBs, and crossing-overs  
334 (involving HR) are required to produce functional gametes (Zhang et al., 2019). By contrast,  
335 somatic DSBs are introduced by accident and such cells are rarely spontaneously confronted to  
336 such high levels of simultaneous DSBs. In our functional test, RAD51 foci assembly by the

337 mutated *BRCA2* was significantly decreased at higher doses (>5 Gy) that generate a high  
338 number of DSBs (with an estimation of 30 to 40 DSB/Gy/mammalian genome (Ruiz de  
339 Almodóvar et al., 1994)). Therefore, the *R2842C-BRCA2* mutation is expected to affect the  
340 processing of such a high number of simultaneous meiotic DSBs, explaining the infertility  
341 observed in our patient.

342 Heterozygous *BRCA2* mutations increase susceptibility to familial breast and ovarian cancer  
343 (Walsh et al., 2011). Such increased susceptibility has not been observed in our patient's family.  
344 The efficient loading of RAD51 on low number of DNA damages in the patient's somatic cells  
345 could explain the absence of somatic pathologies. Although we cannot rule out the possibility  
346 that the patient may develop cancer on the long-term, after triggering by environmental causes,  
347 the fact that neither the patient nor her relatives have yet developed other pathologies implies  
348 that the *BRCA2* mutation is hypomorphic and retains a residual HR activity, as supported by our  
349 functional studies.

350 Recently, two young sisters presenting a syndromic XX ovarian dysgenesis were reported to  
351 carry compound heterozygous C-terminal *BRCA2* truncations. However, in addition to POI,  
352 these patients and their family fulfilled the diagnostic criteria of FA: microcephaly, café-au-lait  
353 spots, childhood leukemia, and a characteristic severe cellular response to mitomycin in  
354 chromosomal breakage tests (over 100 breakages per cells at 150 and 300 nM MMC, 50 times  
355 the number observed in control lymphocytes), the hallmark of FA (Auerbach, 2009; Weinberg-  
356 Shukron et al., 2018). Therefore, these cases are not similar to our patient that presents only an  
357 isolated POI.

358 In conclusion, we describe and functionally characterize here for the first time a homozygous  
359 hypomorphic variant of *BRCA2*, in a patient with isolated POI without somatic pathology in  
360 the patient and her family. The recent implication of DNA repair genes in POI establishes a  
361 genetic link between infertility and cancer. As *BRCA2* is a major susceptibility gene for breast

362 and ovarian cancer, this represents a major ethical issue for the care of these patients. It should  
363 change the genetic counselling and pre-test information for patients with isolated POI and their  
364 families. Indeed, such counselling should be addressed while keeping in mind a possible defect  
365 in major DNA repair genes such as *BRC A2*. More generally, this study has also a wide impact  
366 for the understanding of the processes controlling genome plasticity and the consequences of  
367 their defects, in somatic and germ cells.

368

## 369 **MATERIAL AND METHODS**

### 370 **Ethics statement**

371 The study was approved by all the institutions involved and by the agence de Biomedecine  
372 (reference number PFS12-002). Written informed consent was received from participants prior  
373 to inclusion in the study.

374

### 375 **Whole Exome Sequencing and bioinformatics analysis**

376 WES, reads quality check and mapping was performed by Beckman Coulter Genomics  
377 (Danvers, USA). Exon capture was performed using the hsV5UTR kit target enrichment kit.  
378 Mapping was performed on the GRCh37.p13 reference genome using the Burrows-Wheeler  
379 Alignment tool (BWA) version 0.6.1-r104 with default parameters, and samtools 'Rmdup' was  
380 used to remove duplicates. Prior to variant calling, reads were re-aligned around known or  
381 suspected indels by the GATK Realigner commands. The samtools version 2.0 'mpileup'  
382 command and the bcftools multi-allelic calling model were used for variant calling. Variants  
383 were annotated by SnpEff, VEP (Variant Effect Predictor) and dbNSFP 3.5a. Minor Allele  
384 Frequencies were manually verified using ExAC (<http://exac.broadinstitute.org/>), Gnomad  
385 (<https://gnomad.broadinstitute.org/>) and Kaviar (<http://db.systemsbio.net/kaviar/>)  
386 databases.

387

### 388 **Sanger Sequencing Analysis**

389 To confirm the presence and segregation of the variant, direct genomic Sanger DNA sequencing  
390 of *BRCA2* was performed in the patient and both parents using specific *BRCA2* primers: 5'-  
391 GACTACCCTCTCATAGCTCCAG-3' and 5'-GGAAGAAGCAGGGAACTC-3'

392

### 393 **Protein modelisation**

394 The 1mje and 1miu structures of BRCA2 were retrieved from PDB databank 1. The 1mje  
395 structure was opened in iMol (Piotr Rotkiewicz, "iMol Molecular Visualization Program,"  
396 (2007) <http://www.pirx.com/iMol>) for displaying the proximity of the mutation to the DNA-  
397 binding groove in the C-terminal domain of the BRCA2 protein. The human WT and mutated  
398 sequence were threaded onto the 1miu structure using RaptorX 2, and the resulting pdb  
399 structures were rendered in iMol for displaying the occupancy of lateral chains.

400

### 401 **Collection of human samples**

402 GM3348 (WT1) and GM3652 (WT2) are wild-type primary human fibroblasts (Coriell institute,  
403 Camden, USA). EGF 208\_F, noted as FANCD1 cells, are primary fibroblast from a FANCD1  
404 patient biopsy (generous gift from Dr. Jean Soulier, Hopital St Louis, Paris). Primary fibroblasts  
405 were derived from a skin biopsy of the patient. EBV-immortalized lymphoblastoid cell lines  
406 derived from the patient, both parents and two healthy women as control were established at the  
407 Banque de cellules, Genopole (Evry, France) using a standard protocol.

408

### 409 **Collection of human fetal gonads**



410 Human fetal ovaries were obtained and studied as described (Frydman et al., 2017). Fetal ovaries  
411 were harvested from material obtained following legally induced abortions or therapeutic  
412 terminations of pregnancies at the Department of Obstetrics and Gynecology at the Antoine  
413 Bécclère Hospital, Clamart (France). All women provided an informed consent and this study  
414 was approved by the Biomedicine Agency (reference number PFS12-002). Fetal age was  
415 calculated by measuring the length of limbs and feet according to a developed mathematical  
416 model (Evtouchenko et al., 1996). After collection, fetal gonads were stored in RLT RNA lysis  
417 buffer (Qiagen, Courtaboeuf, France) for gene expression profiling or fixed for histology and  
418 immunostaining. Fetal ovaries from the therapeutic terminations of pregnancies (second and  
419 third trimester of pregnancy) had to display normal histological features before being included  
420 in the study.

421

#### 422 **Detection of BRCA2 in human fetal ovaries**

423 Immunohistochemistry was studied as previously described (Poulain et al., 2015). Fetal human  
424 ovaries were fixed overnight in 10% neutral formalin (Carlo Erba Reagents, Val de Reuil, France)  
425 before being dehydrated, embedded in paraffin wax and cut into 5 $\mu$ m sections. After dewaxing  
426 and rehydration, antigen retrieval was performed in HIER citrate buffer pH 6 (Zytomed,  
427 Diagomics, Blagnac, France) in an autoclave (Retriever 2100, Proteogenix, Mundolsheim,  
428 France). Sections were then bathed in distilled water and incubated for 15 min in 3% H<sub>2</sub>O<sub>2</sub> at  
429 room temperature. After 30 min in 2.5% normal Horse serum (Vector laboratories, Eurobio, Les  
430 Ulis, France), primary antibody diluted in PBS was incubated for 2h at 37°C. The primary  
431 antibody used in this study was rabbit polyclonal to human BRCA2 (1:200, Abcam, Paris,  
432 France). The primary antibody was revealed using the secondary antibody anti-rabbit IgG  
433 (IMPRESS kit, Vector Laboratories, Eurobio). Peroxidase activity was visualized using VIP  
434 (Vector laboratories, Eurobio) as a substrate. Sections were counterstained with hematoxylin.

435

### 436 **Real-time quantitative PCR**

437 In order to measure the expression of multiple genes during human gonadal development, total  
438 RNA from fetal ovaries was extracted using the RNeasy Mini Kit (Qiagen Courtaboeuf, France),  
439 followed by a reverse transcription and whole transcriptome amplification (Quantitect Whole  
440 Transcriptome cDNA Amplification, Qiagen, Courtaboeuf, France). Seventeen ovaries were  
441 included for gene expression profiling as previously described (Poulain et al., 2014). Each RNA  
442 sample was analysed in triplicate. The 7900HT Fast Real-Time PCR System (Applied  
443 Biosystems, Foster City, CA) and SYBR-green labelling were used for quantitative RT-PCR.  
444 The comparative  $\Delta\Delta$ cycle threshold method was used to determine the relative quantities of  
445 mRNA using *ACTB* ( $\beta$ -actin) mRNA as reference gene for normalization. The sequences of  
446 oligonucleotides used with SYBR-green detection were designed with Primer Express Software:

447 *ACTB*: 5'-TGACCCAGATCATGTTTGAGA-3'; 3'-TACGGCCAGAGGCGTACAGG-5'

448 *BRCA2*: 5'-AGACTGTACTTCAGGGCCGTACA-3'; 3'-GCTGAGACAGGTGTGGAAAC-5'.

449 *SYCP3*: 5'-TGCGGTGTGTTTCAGTCAGG-3', 3'-TTTTTCCGGAGGACACCATATT-5'

450

### 451 **Chromosome breakage studies**

452 Chromosome breakage studies were performed in EBV-immortalized lymphoblastoid cell lines  
453 derived from the patient, her mother, a *FANCD1* patient and a healthy woman as control. They  
454 were studied at the Gustave Roussy Institute (Villejuif, France), following a standard in-house  
455 protocol. EBV-immortalized cells were cultured under standard conditions for karyotyping.  
456 DNA damage was induced using Mitomycin C (MMC, Sigma) added for 48h. For each sample,  
457 three conditions were tested: without MMC to analyze spontaneous damages, and with 300 nM  
458 and 1000 nM MMC. Chromosome breakages were scored by an experimented cytogeneticist on  
459 at least 20 metaphases.

460

#### 461 **Cell proliferation assay**

462 Primary fibroblasts from the POI patient, two healthy WT controls (GM3348 and GM3562) and  
463 a FANCD1 patient were seeded into 6-well cell culture and grown in MEM (Gibco, Life  
464 Technologies) supplemented with 20% fetal calf serum (FCS; Lonza Group, Ltd.) and were  
465 incubated at 37°C with 5% CO<sub>2</sub>. For thirteen days, cells were dissociated from wells with trypsin  
466 and counted every 2-3 days using a Z1 Particle Counter (Beckman Coulter).

467

#### 468 **Cell transfection and HR efficiency test**

469 The HR efficiency was assessed in RG37 cell line, derived from SV40-transformed GM639  
470 human fibroblasts in which we stably integrated the pDR-GFP gene conversion reporter (Dumay  
471 et al., 2006; Pierce et al., 1999). RG37 were cultured in DMEM supplemented with 10% fetal  
472 calf serum (FCS) and 2 mM glutamine and were incubated at 37°C with 5% CO<sub>2</sub>. For HR  
473 efficiency test, The I-SceI meganuclease was expressed by transient transfection of the pCMV-  
474 HA-I-SceI expression plasmid (Liang et al., 1998) with Jet-PEI according to the manufacturer's  
475 instructions (Polyplus transfection), and cells were incubated for 48 hours. Cells were collected  
476 in PBS and 50 mM EDTA, pelleted and fixed with 2% paraformaldehyde for 20 minutes. The  
477 percentage of GFP-expressing cells was scored by FACS analysis using a BD Accuri C6 flow  
478 cytometer (BD Biosciences).

479 For silencing experiments, 20000 cells were seeded 1 day before transfection with siRNAs,  
480 using INTERFERin following the manufacturer's instructions (Polyplus Transfection) with 20  
481 nM of one of the following siRNAs: Control (5'-AUGAACGUGAAUUGCUCAA-3'), BRCA2-  
482 3 (5'-GCUUCAGUUGCAUAUCUUA-3'). The BRCA2 siRNA targets the 3'UTR of endogenous  
483 BRCA2 mRNA. All siRNAs were synthesized by Eurofins (France). Forty-eight hours later, the  
484 cells were transfected with the pCMV-HA-I-SceI expression plasmid. At least 3 independent

485 experiments were performed, and HA-I-SceI expression and silencing efficiency were verified  
486 by Western blot as described below.

487

#### 488 **Western blotting**

489 Cells were lysed in buffer containing 20 mM Tris HCl (pH 7.5), 1 mM Na<sub>2</sub>EDTA, 1 mM EGTa,  
490 150 mM NaCl, 1% (w/v) NP40, 1% sodium deoxycholate, 2.5 sodium pyrophosphate, 1 mM β-  
491 glycerophosphate, 1 mM NA<sub>3</sub>VO<sub>4</sub> and 1 μg/ml leupeptin supplemented with complete mini  
492 protease inhibitor (Roche). Denatured proteins (20-40 μg) were electrophoresed in 9% SDS-  
493 PAGE gels or NuPAGE™ 3-8% Tris-Acetate Protein Gels (Invitrogen), transferred onto a  
494 nitrocellulose membrane and probed with specific antibodies: anti-BRCA2 (1/4000, ab9143,  
495 Abcam), anti-Vinculin (1/8000, ab18058 Abcam), and anti-HA (1/1,000, F-7 #sc-7392,  
496 SantaCruz). Immunoreactivity was visualized using an enhanced chemiluminescence detection  
497 kit (ECL, Pierce). The intensity of the bands was quantified by ImageJ.

498

#### 499 **Irradiation**

500 Cells were exposed to 0.5, 1, 2, 5, 6 or 10 Gy IR 24h after seeding using an X-ray source (1.03  
501 Gy/min) (X-RAD 320, Precision X-Ray Inc., North Branford, CT). The cells were fixed with  
502 4% paraformaldehyde 2h, 4h, 6h, 8h or 24h after irradiation, and immunofluorescence was  
503 performed as described below.

504

#### 505 **Immunofluorescence**

506 Cells were seeded onto slides, then washed with PBS, treated with CSK buffer (100 mM NaCl,  
507 300 mM sucrose, 3 mM MgCl<sub>2</sub>, 10 mM Pipes pH 6.8, 1 mM EGTa, 0.2X Triton, and protease  
508 inhibitor cocktail (complete ULTRA Tablets, Roche) and fixed in 2% paraformaldehyde for 15  
509 min. The cells were then permeabilized in 0.5% Triton-X 100 for 5 min, saturated with 2% BSA

510 and 0.05% Tween20 and probed with anti-RAD51 antibody (1/500, PC130, Merck Millipore)  
511 for 2 h at 37°C. After 3 washes in PBS-Tween20 (0.05%) at RT, the cells were probed with  
512 Alexa-coupled anti-mouse or anti-rabbit secondary antibody (1/1,000, Invitrogen) for 1h at  
513 37°C. After 3 washes, the cells were mounted in DAKO mounting medium containing 300 nM  
514 DAPI and visualized using a fluorescence microscope (Zeiss Axio Observer Z1) equipped with  
515 an ORCA-ER camera (Hamamatsu). Image processing and foci counting were performed using  
516 the ImageJ software.

517

### 518 **Statistical Analysis**

519 Statistical analyses were performed using GraphPad Prism 3.0 (GraphPad Software).

520

### 521 **Acknowledgements:**

522 We thank Baptiste Fouquet for help in some experiments, Jean Soulier and the “Cellulothèque  
523 des hémopathies de l’Hôpital Saint-Louis » for the gift of FANCD1 primary fibroblasts and  
524 Alexandra Benachi for fetal ovaries. This study was supported by Université Paris Diderot (SC),  
525 Université Paris Sud-Paris Saclay (ED, AH, MM), by the Agence Nationale de Biomedecine  
526 (AH, MM) and by Institut Universitaire de France (GL). BSL was supported by the Ligue  
527 Nationale contre le cancer “Equipe labellisée 2017”, Agence Nationale de la Recherche (ANR-  
528 16-CE12-0011-02 and ANR-16-CE18-0012-02), AFM-Téléthon and Institut National du  
529 Cancer (INCa-PLBIO18-232).

530

### 531 **Authors contributions**

532 MM, GL and BSL designed research studies. ED, AH, ST and SM conducted experiments. SC,  
533 ED, AH, GL, BSL and MM acquired and analysed data. MM, SC, BSL, AH and GL wrote the  
534 manuscript.

535

536 **Disclosure:**

537 The authors declare no conflict of interest.

538 **REFERENCES**

- 539 AlAsiri S, Basit S, Wood-Trageser MA, Yatsenko SA, Jeffries EP, Surti U, Ketterer DM, Afzal  
540 S, Ramzan K, Faiyaz-Ul Haque M, Jiang H, Trakselis MA, Rajkovic A. 2015. Exome  
541 sequencing reveals MCM8 mutation underlies ovarian failure and chromosomal instability. *J*  
542 *Clin Invest* 125:258–262. doi:10.1172/JCI78473
- 543 Auerbach AD. 2009. Fanconi anemia and its diagnosis. *Mutat Res* 668:4–10.  
544 doi:10.1016/j.mrfmmm.2009.01.013
- 545 Chen J, Silver DP, Walpita D, Cantor SB, Gazdar AF, Tomlinson G, Couch FJ, Weber BL,  
546 Ashley T, Livingston DM, Scully R. 1998. Stable interaction between the products of the  
547 BRCA1 and BRCA2 tumor suppressor genes in mitotic and meiotic cells. *Mol Cell* 2:317–  
548 328.
- 549 Crickard JB, Kaniecki K, Kwon Y, Sung P, Greene EC. 2018. Meiosis-specific recombinase  
550 Dmc1 is a potent inhibitor of the Srs2 antirecombinase. *Proc Natl Acad Sci U S A*  
551 115:E10041–E10048. doi:10.1073/pnas.1810457115
- 552 Dumay A, Laulier C, Bertrand P, Saintigny Y, Lebrun F, Vayssiere JL, Lopez BS. 2006. Bax  
553 and Bid, two proapoptotic Bcl-2 family members, inhibit homologous recombination,  
554 independently of apoptosis regulation. *Oncogene*.
- 555 Evtouchenko L, Studer L, Spenger C, Dreher E, Seiler RW. 1996. A mathematical model for  
556 the estimation of human embryonic and fetal age. *Cell Transplant* 5:453–464.
- 557 Fouquet B, Pawlikowska P, Caburet S, Guigon C, Mäkinen M, Tanner L, Hietala M, Urbanska  
558 K, Bellutti L, Legois B, Bessieres B, Gougeon A, Benachi A, Livera G, Rosselli F, Veitia RA,  
559 Misrahi M. 2017. A homozygous FANCM mutation underlies a familial case of non-  
560 syndromic primary ovarian insufficiency. *eLife* 6. doi:10.7554/eLife.30490
- 561 Frydman N, Poulain M, Arkoun B, Duquenne C, Tourpin S, Messiaen S, Habert R, Rouiller-  
562 Fabre V, Benachi A, Livera G. 2017. Human foetal ovary shares meiotic preventing factors  
563 with the developing testis. *Hum Reprod Oxf Engl* 32:631–642. doi:10.1093/humrep/dew343
- 564 Guidugli L, Pankratz VS, Singh N, Thompson J, Erding CA, Engel C, Schmutzler R, Domchek  
565 S, Nathanson K, Radice P, Singer C, Tonin PN, Lindor NM, Goldgar DE, Couch FJ. 2013. A  
566 classification model for BRCA2 DNA binding domain missense variants based on homology-  
567 directed repair activity. *Cancer Res* 73:265–275. doi:10.1158/0008-5472.CAN-12-2081
- 568 Hoeijmakers JH. 2009. DNA damage, aging, and cancer. *N Engl J Med*.
- 569 Huhtaniemi I, Hovatta O, La Marca A, Livera G, Monniaux D, Persani L, Heddar A, Jarzabek  
570 K, Laisk-Podar T, Salumets A, Tapanainen JS, Veitia RA, Visser JA, Wieacker P, Wolczynski  
571 S, Misrahi M. 2018. Advances in the Molecular Pathophysiology, Genetics, and Treatment of  
572 Primary Ovarian Insufficiency. *Trends Endocrinol Metab* TEM 29:400–419.  
573 doi:10.1016/j.tem.2018.03.010
- 574 Lambert S, Lopez BS. 2000. Characterization of mammalian RAD51 double strand break repair  
575 using non-lethal dominant-negative forms. *EMBO J* 19:3090–3099.  
576 doi:10.1093/emboj/19.12.3090

- 577 Liang F, Han M, Romanienko PJ, Jasin M. 1998. Homology-directed repair is a major double-  
578 strand break repair pathway in mammalian cells. *Proc Natl Acad Sci U S A*.
- 579 Ludwig T, Chapman DL, Papaioannou VE, Efstratiadis A. 1997. Targeted mutations of breast  
580 cancer susceptibility gene homologs in mice: lethal phenotypes of *Brca1*, *Brca2*, *Brca1/Brca2*,  
581 *Brca1/p53*, and *Brca2/p53* nullizygous embryos. *Genes Dev* 11:1226–1241.
- 582 Martinez JS, von Nicolai C, Kim T, Ehlén Å, Mazin AV, Kowalczykowski SC, Carreira A.  
583 2016. BRCA2 regulates DMC1-mediated recombination through the BRC repeats. *Proc Natl*  
584 *Acad Sci U S A* 113:3515–3520. doi:10.1073/pnas.1601691113
- 585 Meyer S, Tischkowitz M, Chandler K, Gillespie A, Birch JM, Evans DG. 2014. Fanconi  
586 anaemia, BRCA2 mutations and childhood cancer: a developmental perspective from clinical  
587 and epidemiological observations with implications for genetic counselling. *J Med Genet*  
588 51:71–75. doi:10.1136/jmedgenet-2013-101642
- 589 Miao Y, Wang P, Xie B, Yang M, Li S, Cui Z, Fan Y, Li M, Xiong B. 2019. BRCA2 deficiency  
590 is a potential driver for human primary ovarian insufficiency. *Cell Death Dis* 10:474.  
591 doi:10.1038/s41419-019-1720-0
- 592 Moynahan ME, Pierce AJ, Jasin M. 2001. BRCA2 is required for homology-directed repair of  
593 chromosomal breaks. *Mol Cell* 7:263–272.
- 594 Pierce AJ, Johnson RD, Thompson LH, Jasin M. 1999. XRCC3 promotes homology-directed  
595 repair of DNA damage in mammalian cells. *Genes Dev* 13:2633–2638.
- 596 Poulain M, Frydman N, Tourpin S, Muczynski V, Souquet B, Benachi A, Habert R, Rouiller-  
597 Fabre V, Livera G. 2015. Involvement of doublesex and mab-3-related transcription factors  
598 in human female germ cell development demonstrated by xenograft and interference RNA  
599 strategies. *Mol Hum Reprod* 21:615. doi:10.1093/molehr/gav029
- 600 Ruiz de Almodóvar JM, Steel GG, Whitaker SJ, McMillan TJ. 1994. A comparison of methods  
601 for calculating DNA double-strand break induction frequency in mammalian cells by pulsed-  
602 field gel electrophoresis. *Int J Radiat Biol* 65:641–649.
- 603 Sharan SK, Morimatsu M, Albrecht U, Lim DS, Regel E, Dinh C, Sands A, Eichele G, Hasty  
604 P, Bradley A. 1997. Embryonic lethality and radiation hypersensitivity mediated by Rad51 in  
605 mice lacking *Brca2*. *Nature* 386:804–810. doi:10.1038/386804a0
- 606 Sharan SK, Pyle A, Coppola V, Babus J, Swaminathan S, Benedict J, Swing D, Martin BK,  
607 Tessarollo L, Evans JP, Flaws JA, Handel MA. 2004. BRCA2 deficiency in mice leads to  
608 meiotic impairment and infertility. *Dev Camb Engl* 131:131–142. doi:10.1242/dev.00888
- 609 Singh TR, Bakker ST, Agarwal S, Jansen M, Grassman E, Godthelp BC, Ali AM, Du C,  
610 Rooimans MA, Fan Q, Wahengbam K, Steltenpool J, Andreassen PR, Williams DA, Joenje  
611 H, de Winter JP, Meetei AR. 2009. Impaired FANCD2 monoubiquitination and  
612 hypersensitivity to camptothecin uniquely characterize Fanconi anemia complementation  
613 group M. *Blood* 114:174–180. doi:10.1182/blood-2009-02-207811
- 614 Souquet B, Abby E, Hervé R, Finsterbusch F, Tourpin S, Le Bouffant R, Duquenne C, Messiaen  
615 S, Martini E, Bernardino-Sgherri J, Toth A, Habert R, Livera G. 2013. MEIOB targets single-



- 616 strand DNA and is necessary for meiotic recombination. *PLoS Genet* 9:e1003784.  
617 doi:10.1371/journal.pgen.1003784
- 618 Tsui V, Crismani W. 2019. The Fanconi Anemia Pathway and Fertility. *Trends Genet TIG*  
619 35:199–214. doi:10.1016/j.tig.2018.12.007
- 620 Tsuzuki T, Fujii Y, Sakumi K, Tominaga Y, Nakao K, Sekiguchi M, Matsushiro A, Yoshimura  
621 Y, Morita T. 1996. Targeted disruption of the Rad51 gene leads to lethality in embryonic  
622 mice. *Proc Natl Acad Sci U S A* 93:6236–6240.
- 623 Walsh T, Casadei S, Lee MK, Pennil CC, Nord AS, Thornton AM, Roeb W, Agnew KJ, Stray  
624 SM, Wickramanayake A, Norquist B, Pennington KP, Garcia RL, King M-C, Swisher EM.  
625 2011. Mutations in 12 genes for inherited ovarian, fallopian tube, and peritoneal carcinoma  
626 identified by massively parallel sequencing. *Proc Natl Acad Sci U S A* 108:18032–18037.  
627 doi:10.1073/pnas.1115052108
- 628 Weinberg-Shukron A, Rachmiel M, Renbaum P, Gulsuner S, Walsh T, Lobel O, Dreifuss A,  
629 Ben-Moshe A, Zeligson S, Segel R, Shore T, Kalifa R, Goldberg M, King M-C, Gerlitz O,  
630 Levy-Lahad E, Zangen D. 2018. Essential Role of BRCA2 in Ovarian Development and  
631 Function. *N Engl J Med* 379:1042–1049. doi:10.1056/NEJMoa1800024
- 632 Wood-Trageser MA, Gurbuz F, Yatsenko SA, Jeffries EP, Kotan LD, Surti U, Ketterer DM,  
633 Matic J, Chipkin J, Jiang H, Trakselis MA, Topaloglu AK, Rajkovic A. 2014. MCM9  
634 mutations are associated with ovarian failure, short stature, and chromosomal instability. *Am*  
635 *J Hum Genet* 95:754–762. doi:10.1016/j.ajhg.2014.11.002
- 636 Yang H, Jeffrey PD, Miller J, Kinnucan E, Sun Y, Thoma NH, Zheng N, Chen P-L, Lee W-H,  
637 Pavletich NP. 2002. BRCA2 function in DNA binding and recombination from a BRCA2-  
638 DSS1-ssDNA structure. *Science* 297:1837–1848. doi:10.1126/science.297.5588.1837
- 639 Yoshida K, Kondoh G, Matsuda Y, Habu T, Nishimune Y, Morita T. 1998. The mouse RecA-  
640 like gene Dmc1 is required for homologous chromosome synapsis during meiosis. *Mol Cell*  
641 1:707–718.
- 642 Zhang J, Fujiwara Y, Yamamoto S, Shibuya H. 2019. A meiosis-specific BRCA2 binding  
643 protein recruits recombinases to DNA double-strand breaks to ensure homologous  
644 recombination. *Nat Commun* 10:722. doi:10.1038/s41467-019-08676-2
- 645

646 **FIGURES SUPPLEMENTS:**

647 **Figure 2–figure supplement 1.**

648 **Whole Exome Sequencing and mapping data for the patient with POI**

Generated reads	% GC	Mapped Reads	Properly Mapped Reads	Reads on Target	Forward Strand	Reverse Strand	Strand Bias	Mapped Pairs	Proper Pairs	Singletons
52,025,212	48%	51,991,410	99.90%	71.20%	50%	50%	0%	99.90%	99%	0%

Read Pairs	Average Coverage	>5X	>10X	Picard duplicates	Samtools duplicates	Median Coverage after removing duplicates
25,967,308	51X	69.9%	67.9%	7.2%	7.2%	42.6X

649

650 [\(Back to main text\)](#)

651

652 **Figure 2–figure supplement 2.**

653 **Filtering of the variants identified by Whole Exome Sequencing in the POI patient**

Variants called in	Patient
<b>Total</b>	<b>219475</b>
SNPs	193442
Indels	26033

Variant filters	# of variants
Minimum depth at variant $\geq 5$	86422
Homozygous	44483
in protein coding gene	21693
in coding sequence or splice	7588
with impact on CDS	4521
not Homozygous in fertile controls	1141
MAF < 1% in GnomAD	10
with pathogenicity predictions	5
with coherent functional information	2

654 *Details about the second variant are provided in the Supplementary Information.*

655 [\(Back to main text\)](#)

656 **Figure 2–figure supplement 3.**

657 **Pathogenicity predictions for the R2842C variant in *BRCA2***

Software	Score for the variant	Pathogenicity threshold	Pathogenicity prediction
SIFT	0	< 0.05	Deleterious
PolyPhen 2	1	> 0.8	Damaging
M-CAP	0.502	> 0.025	Possibly pathogenic
FATHMM-MKL	0.9452	> 0.5	Deleterious
LRT	0.000003	Score is a p-value	Deleterious
MutationTaster	1	0.5	Disease-causing
MutationAssessor	2.67	> 0.65	Medium
FATHMM	-1.88	< -1.5	Deleterious
FATHMM-MKL coding	0.94518	0.5 (default) 0.80 (stringent)	Deleterious
PROVEAN	-2.38	-2.28	Neutral
MetaSVM	0.6583	0	Deleterious
MetaLR	0.7556	0.5	Deleterious
REVEL	0.843	0.5 (default) 0.75 (stringent)	Pathogenic
DANN	0.9990224	0.96	Damaging
CADD	8.14	1.75	Damaging
GERP++ RS	5.1	> 4.4	Highly conserved
phyloP100way_vertebrate	4.63	> 1.6	Highly conserved

658

659 [\(Back to main text\)](#)

660

661 **Figure 2–figure supplement 4.**

662 **Conservation of the mutated BRCA2 Arg 2842 aminoacid across species.**

Human ( <i>Homo sapiens</i> )	MEKTS SGLY I F <b>R</b> NEREEEEKEAAKYVEAQQRLEALFTKIQEE
Mouse ( <i>Mus musculus</i> )	VEKTVSGLY I F <b>R</b> SEREEEEKEALRF AEAQKKLEALFTKVHTE
Naked mole-rat, female ( <i>H. glaber</i> )	MEKTS SGLY I F <b>R</b> NEREEEEKEAAKHAE AQKKLEVLFTKIQGQ
Platypus ( <i>Ornithorhynchus anatinus</i> )	MEKTH TGSYV F <b>R</b> NERAE EKEASKHAESQKKLEALYAKIQDD
Chicken ( <i>Gallus gallus</i> )	MEKTSAGSYV F <b>R</b> NSRAEEREAAKHAEDQKKLEALFAKIQAE
Anole lizard ( <i>Anolis carolinensis</i> )	MEKTS TGSYMF <b>R</b> NCRAEEREAAKHAENKQKTLEALLANIQAE
Chinese softshell turtle ( <i>Pelodiscus sinensis</i> )	VEKMPTGSYV F <b>R</b> NGRAEEREAAKHAENRQKHLEALFSQIQME
Xenopus ( <i>Xenopus tropicalis</i> )	MEKMANGLYV F <b>R</b> NDRAEEREAEKHSANQKKLEMLFSKIQAE
Tetraodon ( <i>Tetraodon nigroviridis</i> )	MERKPEGGTV F <b>R</b> SGRAE EKEARRYNVHKEKAMEILFDKIQAE
Coelacanth ( <i>Latimeria chalumnae</i> )	MEKKSDG I F V F <b>R</b> NDRAEERE AQ RQVENQQRKMESLFAKIQTE
Purple sea urchin ( <i>S. purpuratus</i> )	MEKLPEGGSV F <b>R</b> NAKEEAKAAALHAGRKQNKMEQLFTQIQKQ
Stony coral ( <i>Orbicella faveolata</i> )	MEKMSDGTNV F <b>R</b> NSRLEEREAKKFEADRQKRREKLFKIQEE
Pacific oyster ( <i>Crassostrea gigas</i> )	MEKLPDGGSV F <b>R</b> TAQAE EKFSQLYQKQQDAMESLYRKLEKD
Honey bee ( <i>Apis mellifera</i> )	HEKTSTGES I F <b>R</b> NIRCEEKANI IYEKKCRSMIETFFYAKAEKY
Florida carpenter ant ( <i>Camponotus floridanus</i> )	HEKTASGDS I V <b>R</b> NAKCEEKAQSTYEQCLS KIETFFYANA EKD
Nematode ( <i>Trichinella spiralis</i> )	LEKYADGRSVM <b>R</b> NERCEEQI SLRF AEEVDHLM EKMLERVVND
Thale cress ( <i>Arabidopsis thaliana</i> )	KERLGEKKS I V <b>R</b> SERIE ----SRI IQLHNQRRSALVEGIMCE
Mayze ( <i>Zea Mays</i> )	RERLPDGRFV V <b>R</b> SERMERKALELYHQRVSKIT EDILFEQQEN
Basidiomycete ( <i>Ustilago maydis 521</i> )	VDVDKSNAGAP <b>R</b> GEQEEAEQREAWLQRREDAMQQLELEAEAE

663

664 The sequence of the 42 aa of the BRCA2 Tower domain is shown in 19 different species across

665 a wide evolutionary range. The strict conservation of the arginine residue supports its functional

666 importance.

667

668 [\(Back to main text\)](#)

669

670 **Figure 6-figure supplement 1.**

671 **Whole Exome Sequencing data from the POI patient for all genes included in the FANC**  
 672 **pathway, with the exception of BRCA2, to exclude a potential causative variant in all these**  
 673 **genes.**

Gene name	Alias	Mean Depth in targeted exons (1)	Nb variants in gene (2)	Htz variants (3)	Mean depth at variant positions (4)	Mean ratio for htz allelic reads (5)	Presence of htz variants (6)					Nbr of rare coding variants (7)	
							upstream	5'UTR	deep intronic	3'UTR	downstream	Hmz	and pathogenic
<i>FANCA</i>		65.6	35	31	39.4	1.07	yes	no	yes	yes	yes	0	0
<i>FANCB</i>		63.9	4	4	15.3	1.30	no	yes	yes	no	yes	0	0
<i>FANCC</i>		39.9	0 in this individual										
<i>FANCD1</i>	<i>BRCA2</i>	65.9	13	0	36.8	-	-	-	-	-	-	1	1
<i>FANCD2</i>		73.9	8	7	22.5	0.55	yes	no	yes	no	no	0	0
<i>FANCE</i>		54.2	7	3	30.7	0.85	no	yes	yes	no	no	0	0
<i>FANCF</i>		49.4	2	2	17	0.89	no	no	no	yes	no	0	0
<i>FANCG</i>		73.8	2	2	97.5	0.92	yes	no	yes	no	no	0	0
<i>FANCI</i>		93.6	2	0	33.5	-	-	-	-	-	-	0	0
<i>FANCI</i>	<i>BRIP1</i>	79.7	7	4	42.4	0.95	no	no	yes	yes	no	0	0
<i>FANCL</i>		63.4	2	2	39.5	0.75	no	no	yes	no	no	0	0
<i>FANCM</i>		55.6	0 in this individual										
<i>FANCN</i>	<i>PALB2</i>	97.8	0 in this individual										
<i>FANCO</i>	<i>RAD51C</i>	70.4	0 in this individual										
<i>FANCP</i>	<i>SLX4</i>	61.3	1	1	50	1.13	no	no	no	no	no	0	0
<i>FANCQ</i>	<i>ERCC4</i>	78.2	2	0	17	-	-	-	-	-	-	0	0
<i>FANCR</i>	<i>RAD51</i>	58.5	32	20	30.2	0.94	yes	no	yes	no	no	0	0
<i>FANCS</i>	<i>BRCA1</i>	90.1	16	13	63.4	0.97	yes	no	yes	no	yes	0	0
<i>FANCT</i>	<i>UBE2T</i>	81.0	1	0	26	-	-	-	-	-	-	0	0
<i>FANCU</i>	<i>XRCC2</i>	40.2	0 in this individual										
<i>FANCV</i>	<i>MAD2L2</i>	51.9	4	2	51	1.01	no	no	no	no	yes	0	0
<i>FAAP100</i>	<i>C17orf70</i>	47.7	3	1	31	2.00	no	no	no	no	yes	0	0
<i>FAAP24</i>	<i>C19orf40</i>	83.6	2	0	29.5	-	-	-	-	-	-	0	0
<i>FAAP20</i>	<i>C1orf86</i>	47.2	5	3	32	1.34	no	no	no	no	yes	0	0
<i>FAAP16</i>	<i>APITD1</i>	32.8	0 in this individual										
<i>FAAP10</i>	<i>STRA13</i>	34.9	0 in this individual										
<i>FAN1</i>		85.5	6	6	36.3	1.01	yes	no	no	yes	no	0	0
	mean	64.4	154	101	37.1	1.05							

674

675 (1) For each gene, the mean depth per probe was averaged over all exons of the gene. The good  
 676 coverage for all genes excludes the possibility of not detecting a causative variant in other  
 677 FANC genes.

678 (2) Total number of upstream, downstream, 5' & 3' UTRs, intronic, synonymous, splice site,  
 679 missense, frameshift and stop variants in each gene.

680 (3) The presence of heterozygous variants in a gene excludes the possibility of hemizygoty.

681 (4) For each gene, the mean depth at variant position was averaged for all variants. The good  
682 coverage of variant positions warrants a correct genotyping.

683 (5) The ratio between the number of reads for each allele was averaged for all heterozygous  
684 variants. A ratio close to 1 indicates no bias and argues against a possible deletion of the gene.

685 (6) The presence of heterozygous variants in the various genic portions argues against the  
686 possibility of partial deletions.

687 (7) Among the 154 variants detected in the genes included in the FANC pathway, only the  
688 variant found in BRCA2 is homozygous in the patient, is rare (below 1% in GnomAD database)  
689 and predicted as pathogenic.

690

691 [\*\(Back to main text\)\*](#)

692

693 **Supplementary Information**

694

695 **Variant analysis in the patient with POI**

696 Variants were annotated by SnpEff and VEP and were filtered on the basis of their  
697 homozygosity in the patient, their absence in unrelated fertile in-house controls and a minor  
698 allele frequency (MAF) below 0.01 in all available databases. Further filtering on available  
699 functional data for a possible role in fertility yielded only two plausible candidate variants. The  
700 first variant was a missense rs539695846 in *ARGHEF7*. This gene lies about 250 kb away from  
701 one of the 6 loci identified by genome-wide association study as influencing age at natural  
702 menopause (Stolk et al., 2009). *ARGHEF7* is expressed ubiquitously with a maximum in the  
703 brain, and encodes a cytoplasmic Rho guanine nucleotide exchange factor that plays a role in  
704 cell proliferation, in particular through phosphorylation of FOXO3a (Chahdi and Sorokin,  
705 2008). As *FOXO3a* knockout mice are infertile due to early depletion of the follicle pool  
706 (Castrillon et al., 2003), this regulation could be the basis for a possible role of *ARGHEF7* in  
707 the age of menopause. However, a recent study showed no association between the  
708 polymorphism besides *ARGHEF7* and AMH levels, a reliable marker of ovarian reserve, in  
709 childhood cancer survivors (van Dorp et al., 2013) which lessens the interest of this gene in  
710 fertility.

711 The second variant was the *BRCA2* missense rs80359104 characterized in this study.

712

713 **Targeted Next Generation Study in the mother**

714 The patient's mother had delayed conception followed by secondary amenorrhea at the age of  
715 33 years, not investigated in Turkey. Her amenorrhea, reflecting either a central or peripheral  
716 hypogonadism, could be explained in part by obesity, known to contribute to ovulatory  
717 dysfunction and amenorrhea (Mircea et al., 2007). Thus, we performed a targeted next



718 generation sequencing (NGS) to eliminate other genetic cause that might explain the potential  
719 precocious menopause in the mother. We obtained an average of 1 Gb of sequences with more  
720 than 98% of mappable reads and a mean depth of 150x. Nearly 96% of bases were covered to  
721 a minimum depth of 20x and more than 95% of the read bases had a Qscore of above 30. A  
722 total of four hundred and thirty-seven (437) variants were detected. Twenty variants have a  
723 frequency lower than 2% according to the ExAC base. Six false positive variants were ruled  
724 out with a careful examination of the corresponding BAMs using IGV. Of the 14 remaining  
725 variants, 8 are intronic variants with no predicted effect on splicing. Of the 6 exonic variants,  
726 one is a synonymous variant without impact on splicing. Of the remaining five exonic variants,  
727 4 are predicted to be benign by the M-CAP prediction software (Table S1). The only remaining  
728 variant was the *BRCA2* missense mutation detected in the proband (our patient, Figure 1,  
729 V2), *BRCA2*: c. c.8524C>T; p. Arg2842Cys.  
730 *BRCA2* heterozygous mutations were associated with lower AMH levels, reflecting the ovarian  
731 reserve (Daum et al., 2018). We cannot exclude that the heterozygous *R2842C-BRCA2*  
732 mutation could have an impact on the mother's ovarian reserve in addition to environmental  
733 factors.  
734

735 **Table S1. Rare Variants detected by Targeted Next Generation Sequencing in the mother**

CHR	POS	REF	ALT	AF	Gene	Exon	cDNA	Protein	GnomAD Genome	GnomAD Exome	Kaviar	ACMG	M-CAP
chr13	32945129	C	T	0.500	<b>BRCA2</b> (NM_000059.3)	exon20	c.8524C>T	p.Arg2842Cys	3.24e-05	8.14e-06	.	<b>Pathogenic</b> <b>Supporting</b>	<b>Possibly</b> <b>pathogenic</b>
chr5	140071240	C	G	0.500	HARS2 (NM_012208.3)	exon1	c.7C>G	p.Leu3Val	0.00352	0.00291	0.000643	VUS	Likely benign
chr12	53818988	T	G	0.500	AMHR2 (NM_020547.2)	exon4	c.464T>G	p.Phe155Cys	.	.	.	VUS	Likely benign
chr22	31867903	C	T	0.500	EIF4ENIF1 (NM_019843.3)	exon3	c.97G>A	p.Glu33Lys	0.00452	0.00378	0.0038	Pathogenic Supporting	Likely benign
chr8	31015010	A	G	0.500	WRN (NM_000553.4)	exon33	c.3946A>G	p.Ile1316Val	.	0.000134	0.000161	VUS	Likely benign

736

737 \* VUS: Variant of unknown significance

738 **Supplemental References**

- 739 Castrillon DH, Miao L, Kollipara R, Horner JW, DePinho RA. 2003. Suppression of ovarian  
740 follicle activation in mice by the transcription factor Foxo3a. *Science* **301**:215–218.  
741 doi:10.1126/science.1086336
- 742 Chahdi A, Sorokin A. 2008. Endothelin-1 couples betaPix to p66Shc: role of betaPix in cell  
743 proliferation through FOXO3a phosphorylation and p27kip1 down-regulation independently  
744 of Akt. *Mol Biol Cell* **19**:2609–2619. doi:10.1091/mbc.e07-05-0424
- 745 Daum H, Peretz T, Laufer N. 2018. BRCA mutations and reproduction. *Fertil Steril* **109**:33–  
746 38. doi:10.1016/j.fertnstert.2017.12.004
- 747 Mircea CN, Lujan ME, Pierson RA. 2007. Metabolic fuel and clinical implications for female  
748 reproduction. *J Obstet Gynaecol Can JOGC J Obstet Gynecol Can JOGC* **29**:887–902.  
749 doi:10.1016/S1701-2163(16)32661-5
- 750 Stolk L, Zhai G, van Meurs JBJ, Verbiest MMPJ, Visser JA, Estrada K, Rivadeneira F,  
751 Williams FM, Cherkas L, Deloukas P, Soranzo N, de Keyzer JJ, Pop VJM, Lips P, Lebrun  
752 CEI, van der Schouw YT, Grobbee DE, Witteman J, Hofman A, Pols HAP, Laven JSE,  
753 Spector TD, Uitterlinden AG. 2009. Loci at chromosomes 13, 19 and 20 influence age at  
754 natural menopause. *Nat Genet* **41**:645–647. doi:10.1038/ng.387
- 755 van Dorp W, van den Heuvel-Eibrink MM, Stolk L, Pieters R, Uitterlinden AG, Visser JA,  
756 Laven JSE. 2013. Genetic variation may modify ovarian reserve in female childhood cancer  
757 survivors. *Hum Reprod Oxf Engl* **28**:1069–1076. doi:10.1093/humrep/des472
- 758